PHYSICAL REVIEW VOLUME 182, NUMBER 1 5 JUNE 1969

Generalized Hydrodynamics and Time Correlation Functions

Chang-Hyun Chung and Sidney Yip
Department of Nuclear Engineering, Massachusetts Institute of Technology, Cambridge, Massachusetts 02139
(Received 23 January 1969)

Time correlation functions in classical liquids at high frequencies (10^{12} sec^{-1}) and short wavelengths (10^{-8} cm) are analyzed using linear response theory of Martin and Kadanoff. Rigorous expressions, based on dispersion relation, sum rules, and limiting behavior at long wavelengths and low frequencies, are obtained in terms of damping (or memory) function. Specific assumptions regarding the damping function then enable numerical results to be obtained which are compared with computer molecular-dynamics experiments and inelastic neutron-scattering on liquid argon. It is shown that all the known characteristic features of density and current correlations are reproduced using a Lorentzian frequency dependence of the damping function. In particular, the frequency wave-number relation for excitations described by the longitudinal current correlation is in quantitative agreement with the computer calculations. Relaxation times are derived from the computer results on transverse and longitudinal current correlations, and the van Hove self-(test-particle) correlation. These times exhibit significant variation with wavelength, and all have magnitudes of approximately 1×10^{-13} sec. Present analysis is also applicable to slow neutron-scattering experiments. Coherent- and incoherent-scattering contributions in argon are computed without any adjustable parameter, and the theoretical absolute-scattering intensities are in quite good agreement with experimental data.

I. INTRODUCTION

In the study of atomic and molecular processes in liquids, many phenomena can be discussed in terms of time correlation functions which describe the decay of fluctuations in an equilibrium system.[1-3] Correlation function analyses are therefore of considerable interest because they can be subjected to a variety of experimental tests. The basic properties of time correlation functions are by now well known in the recent literature. These include expressions for transport coefficients, molecular formulas for various sum rules, and hydrodynamic behavior. Correlation functions are equally suitable for investigating dynamical processes in a system not in local thermodynamic equilibrium. Such processes involve wavelengths and frequencies comparable to interatomic distances and microscopic relaxation rates, and at present they are still incompletely understood. In the language of kinetic theory, this range of frequencies and wavelengths constitute the "transition" region.

The experimental methods which can provide information about correlation functions in the transition region are inelastic neutron scattering and computer molecular-dynamics calculations. The density correlation function and the longitudinal current correlation function (see Sec. II for definitions) are directly observable by coherent neutron scattering, whereas the van Hove self-correlation function, which reflects the motion of a test particle, can be studied by incoherent scattering.[4-6] Early interest in neutron studies was mostly concerned with the process of self-diffusion in liquids. For example, neutron experiments were the first to reveal in detail that atoms in a liquid actually perform several localized vibrations before undergoing diffusion. More recently, however, attention is being directed to the problem of cooperative modes. From a number of coherent spectra, dispersion curves have been observed[7,8] and they provided the initial evidence that collective density oscillations occur even at wavelengths comparable to interatomic distances.

The information inferred from neutron measurements, which is often only semiquantitative, has been put into much sharper focus by Rahman through a series of computer molecular-dynamics experiments on liquid argon.[9-12] Rahman has generated all the correlation functions of interest under conditions of known interaction potential and equilibrium structure. Since the computer data do not suffer from difficulties associated with laboratory experiments, they are very useful for testing current theories.

The purpose of this paper is to present a detailed analysis of those correlation functions which have been obtained by computer experiments and inelastic neutron scattering.[13] The calculations are based on the correlation-function formalism developed by Martin and Kadanoff[2,14] and involve specific assumptions which are necessary to obtain numerical results. The validity of these assumptions for liquid argon is examined quantitatively using the available computer and neutron

data.

In the present work each correlation-function calculation is reduced to the problem of determining a frequency and wavelength dependent damping function. This is achieved through the use of a dispersion relation which ensures that the correlation-function expressions will have the correct hydrodynamic limits, and which leads naturally to sum-rule conditions on the damping function. In addition to the moment requirements which can be expressed in terms of interaction potential and equilibrium distribution functions, the damping function is also constrained to give the proper transport coefficient in the low-frequency and long-wavelength limit. As we will see, the advantage of this approach is that even simple assumptions regarding the damping function, so long as its known properties are not violated, can lead to quite reasonable results for the correlation function.

The essential elements of Martin's formalism are summarized in the next section where we introduce the necessary definitions and relations for subsequent calculations. The transverse current correlation, the van Hove self-correlation, and the longitudinal current correlation are analyzed in Secs. III through V. In each case numerical results for argon are obtained and compared with the computer data. In Sec. VI we consider the density correlation function and the interpretation of recent neutron-scattering experiments. Absolute intensity calculations which require no adjustable parameters are presented and shown to be in good agreement with measurements. The overall results are then discussed in the final section where a number of concluding remarks are offered.

II. DEFINITIONS AND BASIC FORMALISM

In this section we define the various correlation and response functions, indicate their properties and interrelations, and describe the basic approach used in subsequent calculations. The dynamical variables we shall be concerned with are the particle and current densities. It is convenient to consider these densities in the form

$$n(\vec{\kappa},t)=N^{-1/2}\sum_{l=1}^{N} e^{i\vec{\kappa}\cdot\vec{r}_l(t)}, \tag{2.1}$$

$$\vec{j}(\vec{\kappa},t)=N^{-1/2}\sum_{l=1}^{N} \vec{v}_l(t)e^{i\vec{\kappa}\cdot\vec{r}_l(t)}, \tag{2.2}$$

where $\vec{r}_l(t)$ and $\vec{v}_l(t)$ are the position and velocity of the lth particle at time t in an N-particle system. The time correlation functions are defined by

$$C(\kappa,t)=\langle A(\vec{\kappa},t)A(-\vec{\kappa},0)\rangle, \tag{2.3}$$

where A is either n or $\vec{j}$, and $\langle X\rangle$ denotes the average of X over an equilibrium distribution function. Because of translational and rotational invariance in a liquid, C depends only on the magnitude of $\vec{\kappa}$ and not its direction. In the case of current-current correlation we decompose the second rank tensor into longitudinal and transverse components,

$$\langle j_\alpha(\vec{\kappa},t)j_\beta(-\vec{\kappa},0)\rangle = \frac{\kappa_\alpha\kappa_\beta}{\kappa^2}J_l(\kappa,t)+\left(\delta_{\alpha\beta}-\frac{\kappa_\alpha\kappa_\beta}{\kappa^2}\right)J_t(\kappa,t), \tag{2.4}$$

and analyze J_l and J_t separately.

Since a number of different correlation functions will be considered, we will use a generic notation in the present discussion and summarize the specific cases in Table I. Besides the density-density correlation, S, the current correlations, J_l and J_t, we also want to discuss the self- (or test-particle) correlation function, S_S, which occurs in the theory of incoherent neutron scattering.[4] Having defined $C(\kappa,t)$ we shall denote by $C(\kappa,\omega)$ its frequency spectrum,

$$C(\kappa,\omega)=\frac{1}{2\pi}\int_{-\infty}^{\infty}dt\,e^{i\omega t}C(\kappa,t) = \frac{1}{\pi}\int_0^{\infty}dt\cos\omega t\,C(\kappa,t). \tag{2.5}$$

Notice that in classical calculations the correlation function is real and even in time.

The approach we use to evaluate the above correlation functions is essentially a linear response theory in which one begins with a complex susceptibility,[2,15]

$$\chi(\kappa,z)=\int_{-\infty}^{\infty}\frac{d\omega'}{\pi}\frac{\chi''(\kappa,\omega')}{\omega'-z}, \tag{2.6}$$

where z is a complex variable. The response function χ'' is defined by

$$\chi''(\kappa,\omega)=\int_{-\infty}^{\infty}dt\,e^{i\omega t} \times(i/2)\langle[A(\vec{\kappa},t),A(-\vec{\kappa},0)]_{\mathrm{PB}}\rangle, \tag{2.7}$$

where the bracket $[\ ,\ ]_{\mathrm{PB}}$ denotes Poisson bracket. It follows then that as $z\to\omega+i\epsilon$,

$$\chi(\kappa,\omega)=\mathcal{P}\int_{-\infty}^{\infty}\frac{d\omega'}{\pi}\frac{\chi''(\kappa,\omega')}{\omega'-\omega}+i\chi''(\kappa,\omega), \tag{2.8}$$

where $\mathcal{P}$ denotes the principal value integral. With $z=0$, Eq. (2.6) gives a sum rule which can be worked out for all the cases of interest (see

TABLE I. Notations for various correlation functions and associated quantities.

	Transverse current	Longitudinal current	van Hove (test particle)	Density[a]
$C(\kappa,t)$	$J_t(\kappa,t)$	$J_l(\kappa,t)$	$\langle e^{i\vec{\kappa}\cdot\vec{r}_l(t)} e^{-i\vec{\kappa}\cdot\vec{r}_l(0)}\rangle$	$\langle n(\kappa,t)n(-\kappa,0)\rangle/n$
$C(\kappa,\omega)$	$J_t(\kappa,\omega)$	$J_l(\kappa,\omega)$	$S_s(\kappa,\omega)$	$S(\kappa,\omega)$
$\chi''(\kappa,\omega)$	$\chi''t(\kappa,\omega)$	$\chi_l''(\kappa,\omega)$	$\chi_s''(\kappa,\omega)$	$\chi_{nn}''(\kappa,\omega)$
$D'(\kappa,\omega)$	$D_t'(\kappa,\omega)$	$D_l'(\kappa,\omega)$	$D_s'(\kappa,\omega)$	...
$\chi(\kappa,0)$	mn	mn	β	$n\beta S(\kappa)$
$C_0^2(\kappa)$	0	$[\beta m S(\kappa)]^{-1}$	0	...
$\langle\omega^n(\kappa)\rangle \equiv \int_{-\infty}^{\infty} \frac{\chi''(\kappa,\omega)}{\chi(\kappa,0)}\omega^{n-1}\frac{d\omega}{\pi}$	$\langle\omega_t^n(\kappa)\rangle$	$\langle\omega_l^n(\kappa)\rangle$	$\langle\omega_s^n(\kappa)\rangle$	$\langle\omega_{nn}^n(\kappa)\rangle$

[a]To calculate χ_{nn}'' we first obtain χ_l'' and then use (2.21).

Table I). Now one writes a dispersion relation for $\chi(\kappa,z)$,

$$z^2[1-\chi(\kappa,0)/\chi(\kappa,z)]^{-1} = C_0^2(\kappa)\kappa^2 - iz\kappa^2 D(\kappa,z)\,, \tag{2.9}$$

from which we see

$$C_0^2(\kappa) = \lim_{z\to 0}\frac{z^2}{\kappa^2}\left[1-\frac{\chi(\kappa,0)}{\chi(\kappa,z)}\right]^{-1}. \tag{2.10}$$

The complex damping function $D(\kappa,z)$ is also defined through (2.9); however, we will introduce another function D' which is real and even in ω,

$$D(\kappa,z) = \int_{-\infty}^{\infty}\frac{d\omega'}{\pi i}\frac{D'(\kappa,\omega')}{\omega'-z}\,. \tag{2.11}$$

There are two important consequences of (2.9). First, it implies the following relation between the response function and the damping function $D'(\kappa,\omega)$,

$$\frac{\chi''(\kappa,\omega)}{\chi(\kappa,0)} = \omega^3\kappa^2 D'(\kappa,\omega)\left[\left(\omega^2 - C_0^2(\kappa)\kappa^2 + \kappa^2\omega^2\mathcal{P}\int_{-\infty}^{\infty}\frac{d\omega'}{\pi}\frac{D'(\kappa,\omega')}{\omega'^2-\omega^2}\right)^2 + [\omega\kappa^2 D'(\kappa,\omega)]^2\right]^{-1}. \tag{2.12}$$

Secondly, using (2.6), (2.9), and (2.11) and making a large z expansion, one obtains relations between the frequency moments of χ'' and D'. The first-two relations are

$$\frac{\langle\omega^2(\kappa)\rangle}{\kappa^2} = C_0^2(\kappa) + \int_{-\infty}^{\infty}\frac{d\omega}{\pi}D'(\kappa,\omega) \tag{2.13}$$

$$\frac{\langle\omega^4(\kappa)\rangle}{\kappa^2} = C_\infty^4(\kappa)\kappa^2 + \int_{-\infty}^{\infty}\frac{d\omega}{\pi}\omega^2 D'(\kappa,\omega)\,. \tag{2.14}$$

As is well known, the frequency moments of χ'' are equilibrium properties of the liquid which, in principle, can be computed given the interatomic potential and the equilibrium distribution functions.[16,17] For current correlations, explicit expressions have been derived up to $\langle\omega^4(\kappa)\rangle$. Since longitudinal current correlation and density correlation are simply related [see (2.21)], this means that the sixth frequency moment of $S(\kappa,\omega)$ are known. In addition, the corresponding moment for $S_s(\kappa,\omega)$ has been given by Nijboer and Rahman.[10] Numerical computations of these moments at finite κ have been restricted to the fourth moments of the density correlation and the second moments of the current correlation. The fourth moment of the current correlation is given by a fivefold integral which presents a considerable computational problem. However, at $\kappa=0$ the expression reduces to a triple integral which has been evaluated in the case of argon.[16] For explicit expressions for the various moments the reader is referred to the literature. Notice that by defining

$$\kappa^{-2}\langle\omega_t^2(\kappa)\rangle = G_\infty(\kappa)/mn\,, \tag{2.15}$$

$$\kappa^{-2}\langle\omega_l^2(\kappa)\rangle = [\tfrac{4}{3}G_\infty(\kappa)+K_\infty(\kappa)]/mn\,, \tag{2.16}$$

we can identify $G_\infty(\kappa)$ and $K_\infty(\kappa)$ as wavelength dependent high-frequency shear and bulk moduli.[18]

In addition to frequency moments we have constraints on $D'(\kappa,\omega)$ through the relations between response functions and transport coefficients. These may be expressed as[2,14]

$$\lim_{\omega\to 0}\lim_{\kappa\to 0}\left[\frac{\omega}{\kappa^2}\chi_t''(\kappa,\omega)\right]=mnD_t'(0,0)=\eta\ , \quad (2.17)$$

$$\lim_{\omega\to 0}\lim_{\kappa\to 0}\left[\frac{\omega}{\kappa^2}\chi_l''(\kappa,\omega)\right]=mnD_l'(0,0)=\tfrac{4}{3}\eta+\zeta\ , \quad (2.18)$$

$$\frac{1}{\beta}\lim_{\omega\to 0}\lim_{\kappa\to 0}\left[\frac{\omega}{\kappa^2}\chi_s''(\kappa,\omega)\right]=D_s'(0,0)=D\ , \quad (2.19)$$

where η and ζ are the shear and bulk viscosities, and D is the self-diffusion coefficient. Furthermore, we know that

$$\lim_{\kappa\to 0}\left[\frac{\omega}{\kappa^2}\chi_s''(\kappa,\omega)\right]=f(\omega)\ , \quad (2.20)$$

where $f(\omega)$ is the spectrum of the velocity autocorrelation function.[5,19]

There exist several useful relations among the various $C(\kappa,\omega)$ and $\chi''(\kappa,\omega)$. The connection between correlation and response functions is most readily established through the fluctuation-dissipation theorem.[20] Specifically, we have the classical relations,

$$\chi_{nn}''(\kappa,\omega)=\eta\beta\pi\omega S(\kappa,\omega)$$

$$=(\kappa/m\omega)^2\chi_l''(\kappa,\omega)\ , \quad (2.21)$$

$$J_l(\kappa,\omega)=\frac{\kappa^2}{\beta m^2 n\pi}\,\frac{\chi_l''(\kappa,\omega)}{\omega}\ , \quad (2.22)$$

$$J_t(\kappa,\omega)=\frac{\kappa^2}{\beta m^2 n\pi}\,\frac{\chi_t''(\kappa,\omega)}{\omega}\ , \quad (2.23)$$

$$\chi_s''(\kappa,\omega)=\beta\pi\omega S_s(\kappa,\omega)\ . \quad (2.24)$$

In (2.21) the continuity equation

$$i\omega n(\vec{\kappa},\omega)-i\vec{\kappa}\cdot\vec{j}(\vec{\kappa},\omega)=0 \quad (2.25)$$

has been used to relate χ_l'' and χ_{nn}''.

In what follows we will attempt to evaluate χ'' by assuming simple frequency dependence for the corresponding D'. The assumed form of $D'(\kappa,\omega)$ will contain parameters which can be κ-dependent and these will be determined by the sum-rule relations as well as the constraint at small κ and ω. The advantage of this approach is that we anticipate that it is simpler to deal with D' since it approaches a constant in the limit of small κ and ω. The dispersion relation form for χ'' guarantees that it will reduce to the proper hydrodynamic limit, and by using the sum rules one is effectively interpolating between the small and the large κ and ω regions.

III. TRANSVERSE CURRENT CORRELATION

In Sec. II we have reduced the problem of calculating correlation functions to the determination of the damping function $D'(\kappa,\omega)$. Formally D' is defined in terms of χ'', but neither this definition nor a molecular expression is very useful for actual computations. Instead we consider a phenomenological approach in which we postulate a convenient form for the damping function, and try to satisfy as many as possible the properties of D' described in Sec. II.

To motivate our approximation we observe that $D_t'(\kappa,\omega)$ can be regarded as the frequency transform of an appropriate time correlation function. Suppose we assume the latter relaxes exponentially in time, then this implies that D_t' is a Lorentzian,

$$D_t'(\kappa,\omega)=\frac{[\langle\omega_t^2(\kappa)\rangle/\kappa^2]\,\tau_t(\kappa)}{1+\omega^2\tau_t^2(\kappa)}\ . \quad (3.1)$$

This simple form enables us to satisfy the sum rule (2.13) but not (2.14). The wavelength-dependent relaxation time, $\tau_t(\kappa)$, is unspecified except for its limiting value at $\kappa=0$. From (2.17) we have

$$\tau_t(0)=\eta/G_\infty(0)\ . \quad (3.2)$$

The $\kappa=0$ limit of (3.1) is familiar in viscoelasticity where $D_t'(0,\omega)$ is a frequency-dependent shear viscosity and $\tau_t(0)$ is the Maxwell relaxation time.[18,21] At the opposite limit of short wavelengths one can show that the transverse current correlation $J_t(\kappa,\omega)$ should decay like

$$\exp[-\omega^2/(\kappa v_0)^2]\ , \quad \text{where } v_0=(2k_bT/m)^{1/2};$$

v_0 is the thermal speed of the particles. Thus qualitatively we expect $\tau_t(\kappa)$ to behave like $(\kappa v_0)^{-1}$ at large κ. Aside from the limiting behavior, not much is known about $\tau_t(\kappa)$.

The use of (3.1) leads to a very simple form for the current correlation function. Combining (2.12) and (2.23) we have

$$J_t(\kappa,\omega)=(\kappa^2/\pi\beta m)\times\frac{\langle\omega_t^2(\kappa)\rangle/\tau_t(\kappa)}{[\omega^2-\langle\omega_t^2(\kappa)\rangle]^2+[\omega/\tau_t(\kappa)]^2}\ . \quad (3.3)$$

If the relaxation time is also specified we can compare (3.3) with the spectral densities derived from computer molecular-dynamics experiment. As a first approximation we might replace $\tau_t(\kappa)$ by an appropriate constant. If we use (3.2) for this constant, then it would ensure that the cor-

rect hydrodynamic behavior is preserved. Alternatively, the sum rules can be used to estimate the relaxation time.[22] Assuming that D_t' has a Gaussian frequency dependence, one can derive from (2.13) and (2.14) the relation

$$\tau_t^2(\kappa)=\frac{\pi}{2}\,\frac{\langle\omega_t^2(\kappa)\rangle/\kappa^2}{\langle\omega_t^2(\kappa)\rangle/k^2-\kappa^2[\langle\omega_t^2(\kappa)\rangle/\kappa^2]^2} \tag{3.4}$$

Although the molecular expression for $\langle\omega_t^4(\kappa)\rangle/\kappa^2$ is known, it has not been evaluated except at $\kappa=0$.[16] Nevertheless, the replacement of $\tau_t(\kappa)$ by τ_t, the $\kappa=0$ limit of (3.4), is not an unreasonable approximation at finite κ since sum-rule calculations tend to emphasize the high frequency behavior of correlation functions.

One way of studying the validity of (3.3) is to examine the frequency where $J_t(\kappa,\omega)$ has a peak. From his computer data on argon at 76°K and 1.407 g/cm^3, Rahman[12] has observed that J_t has its maximum at a nonzero frequency, which we shall denote as $(\omega_t)_{\max}$, when the wave number exceeds a certain value. Physically, this corresponds to the phenomenon of shear wave propagation in the liquid at high frequencies and short wavelengths. Figure 1 shows Rahman's data and the results obtained using (3.3) and various prescriptions for $\tau_t(\kappa)$. From the observed value of shear viscosity[23] and the calculated value of shear modulus,[24] we find $\tau_t(0)=0.298\times10^{-12}$ sec. Putting this in place of $\tau_t(\kappa)$ in (3.3) leads to $(\omega_t)_{\max}$ values which are in agreement with computer data for $\kappa\lesssim1$. At larger κ the peak frequency becomes too large. Using the transverse current sum rules computed by Forster *et al.*,[16] we obtain from the $\kappa\to0$ limit of (3.4) $\tau_t=0.135\times10^{-12}$ sec. As shown in Fig. 1 this value leads to a reasonable prediction of $(\omega_t)_{\max}$ for $\kappa\gtrsim1$. The discrepancy in this region can be partly reduced by using τ_t in a simple interpolation scheme, i.e.,

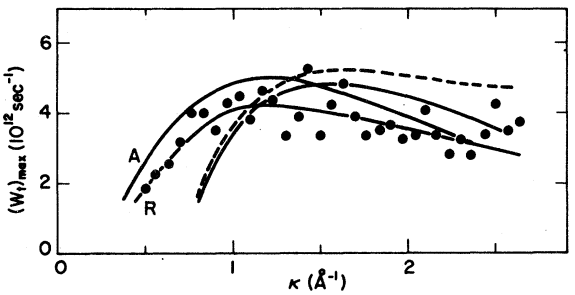

FIG. 1. Dispersion in excitation frequency of transverse current correlations in liquid argon. Theoretical results obtained with various prescriptions of the shear relaxation time are dashed curve [constant τ_t given by $\kappa=0$ limit of (3.4)], solid curve [$\tau_t(\kappa)$ from (3.5)], and the solid curve A [$\tau_t(\kappa)$ from (3.6)]. Curve R is drawn through the computer points of Rahman, its use is described in the text.

$$\tau_t^{-2}(\kappa)=1/\tau_t^2+(\kappa v_0)^2\,. \tag{3.5}$$

The fact that the theoretical values deviate appreciably at small wave numbers is not surprising because we know that as $\kappa\to0$ our prescription would give a shear viscosity about half of the observed value. We conclude therefore that in the context of the single relaxation-time approximation, (3.1), $\tau_t(\kappa)$ ought to have significant wavelength dependence. It should start at about 0.298×10^{-12} at $\kappa=0$, at $\kappa=1$ it should decrease by more than a factor of 2, and it should show a gradual decrease with further increase in wave number.

Akcasu and Daniels have recently proposed a method of computing $\tau_t(\kappa)$.[25] The argument is essentially based on the requirement that as $\kappa\to\infty$, the peak frequency $(\omega_t)_{\max}$ should vanish like the free-particle result. This approach yields a $\tau_t(\kappa)$ having the form

$$\tau_t^{-2}(\kappa)=2\langle\omega_t^2(\kappa)\rangle+\frac{\tau_t^{-2}(0)+(\kappa v_0)^2-2\langle\omega_t^2(\kappa)\rangle}{1+(\kappa/\kappa_0)^2} \tag{3.6}$$

where κ_0 is a parameter. Using $\kappa_0=1.5$ Å^{-1} one obtains the result labeled A in Fig. 1.

The simplicity of (3.3) makes it possible to reverse the procedure and use the computer data to derive the relaxation time $\tau_t(\kappa)$. From (3.3) we have

$$\tau_t^{-2}(\kappa)=2[\langle\omega_t^2(\kappa)\rangle-(\omega_t)^2_{\max}]\,. \tag{3.7}$$

Drawing a smooth curve (labeled R in Fig. 1) through the computer points and using (3.7) we obtain the curve labeled R in Fig. 2. The various approximations just described are also shown for comparison. It can be seen that the optimum value for the parameter κ_0 in the Akcasu prescription should be about 1.5 or somewhat lower.

Once $\tau_t(\kappa)$ is determined we can go back and analyze the spectral density $J_t(\kappa,\omega)$ itself and the corresponding time correlation function,

$$J_t(\kappa,t)=(\kappa^2/\beta m)e^{-t/\tau_t(\kappa)}\times\left(\cos\Omega(\kappa)t+\frac{1}{2\tau_t(\kappa)\,\Omega(\kappa)}\sin\Omega(\kappa)t\right) \tag{3.8}$$

with $\Omega^2(\kappa)=\langle\omega_t^2(\kappa)\rangle-\frac{1}{4}\tau_t^{-2}(\kappa)$.

The theoretical results obtained using (3.5) are shown as dashed curves in Fig. 3, but in Fig. 4

they are drawn as solid curves. The computer data are denoted by the solid curves in Fig. 3 and in Fig. 4 they appear as points. The points in Fig. 3 correspond to $\tau_t(\kappa)$ values taken from the curve labeled R in Fig. 2. The discrepancy which still remains when the optimum relaxation-time values are used must then be attributed to the assumption of (1). In Fig. 4 the dashed curves correspond to (3.8) with $\tau_t(\kappa)$ given by (3.6), whereas the solid curves are obtained using (3.5). From these results we see that (3.5) is a semiquantitatively useful approximation for $\kappa \gtrsim 1$. At longer wavelengths the initial decay given by (3.5) is too slow, which is consistent with the underestimate of the shear viscosity.

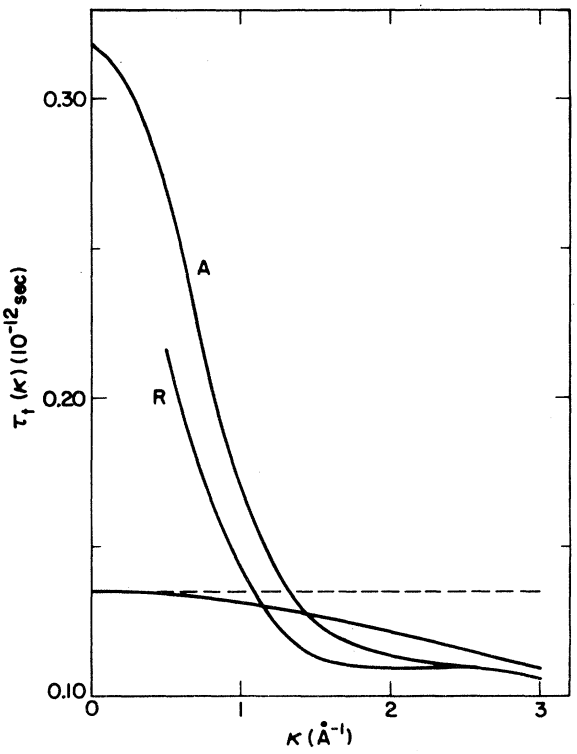

FIG. 2. Variation with wave number of shear relaxation time in liquid argon. Curve R is derived from the computer $(\omega_t)_{\max}$ (curve R in Fig. 1). Curve A corresponds to (3.6), and the solid curve corresponds to (3.5) with τ_t equal to 1.35×10^{-13} sec.

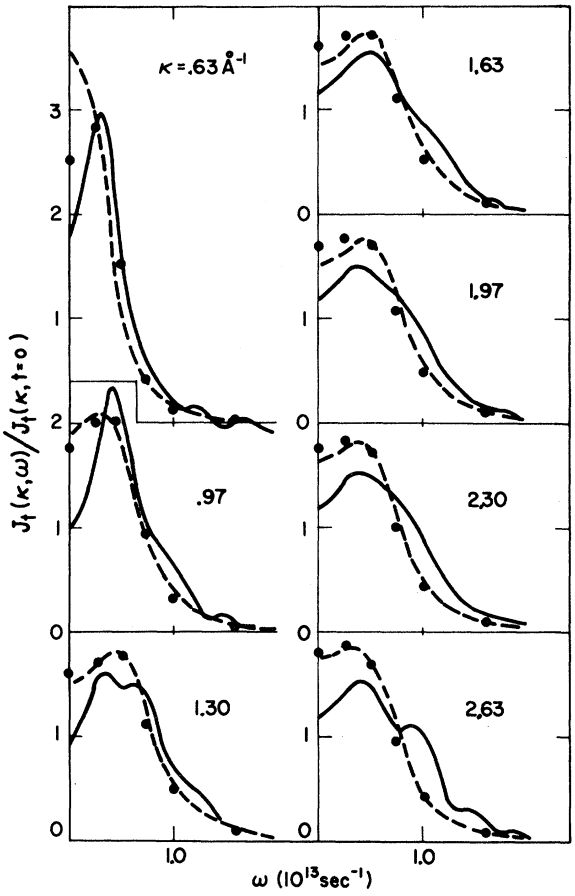

FIG. 3. Spectral densities of transverse current correlations in liquid argon (in units of $10^{-13}/\pi$ sec), with $J_t(\kappa, t=0) = \kappa^2/m\beta$. Solid curves are computer results while the calculations are denoted by dashed curves [$\tau_t(\kappa)$ from (3.5)] and points [$\tau_t(\kappa)$ given by curve R in Fig. 2].

IV. VAN HOVE SELF-CORRELATION FUNCTION

The correlation function $S_S(\kappa, \omega)$ resembles the transverse current correlation $J_t(\kappa, \omega)$ in that both are characterized by a nonpropagating hydrodynamic mode in the limit of small κ and ω. The analog of shear viscosity in the S_S calculation is of course the self-diffusion coefficient.[26] To find $D_S'(\kappa, \omega)$ we have the sum rules from (2.13) and (2.14),[16]

$$\langle \omega_S^2(\kappa)\rangle/\kappa^2 = \int_{-\infty}^{\infty} \frac{d\omega}{\pi} D_S'(\kappa, \omega) = (\beta m)^{-1}, \tag{4.1}$$

$$\langle \omega_S^4(\kappa)\rangle/K^2 = \int_{-\infty}^{\infty} \frac{d\omega}{\pi} \omega^2 D_S'(\kappa, \omega) + (\kappa/\beta m)^2 = 3(\kappa/\beta m)^2 + (3\beta m^2)^{-1}\langle \nabla^2\phi(r)\rangle, \tag{4.2}$$

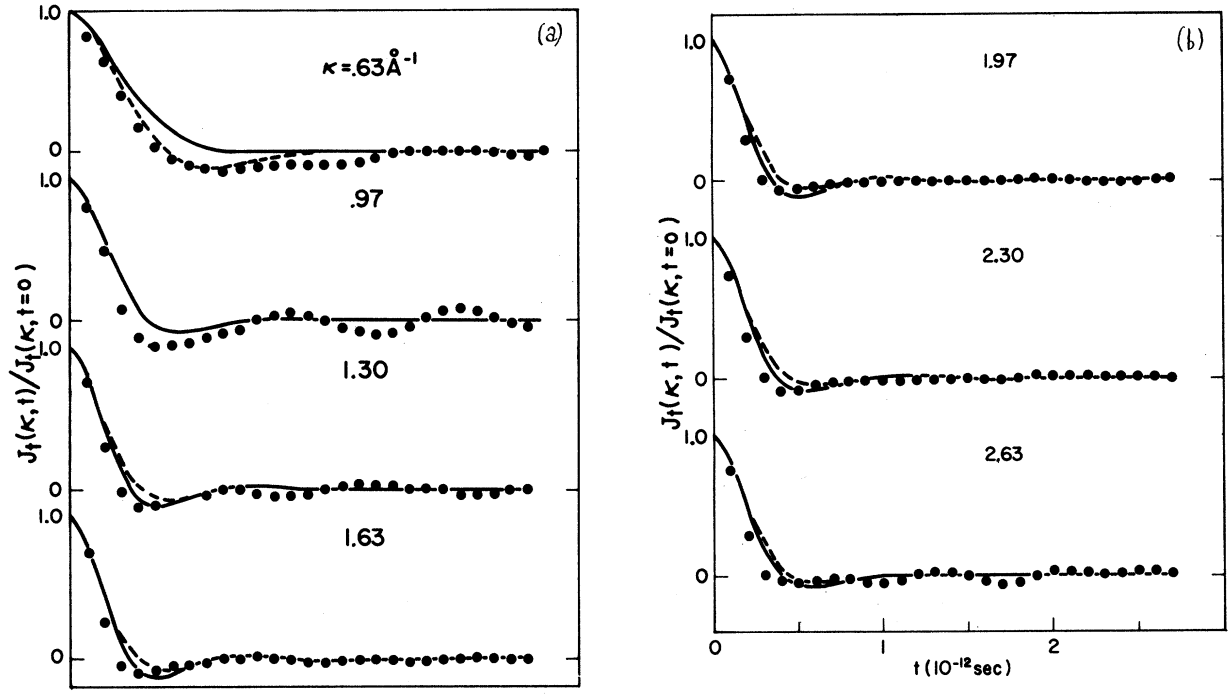

FIG. 4. Transverse current correlations in liquid argon. Theoretical results are shown as solid curves [$\tau_t(\kappa)$ from (3.5)] and dashed curves [$\tau_t(\kappa)$ from (3.6)]. The points denote computer data.

with $\frac{1}{3}\langle \nabla^2\phi(r)\rangle = n\int d^3r g_2(r)(\hat{\kappa}\cdot\vec{\nabla})^2\phi(r)$. (4.3)

From (2.20) we can interpret $D_S'(0,\omega)\beta$ as $f(\omega)$, the spectral density of the velocity autocorrelation function.[19] The single relaxation-time approximation becomes in this case

$$D_S'(\kappa,\omega) = [\tau_S(\kappa)/\beta m]/[1+\omega^2\tau_S^2(\kappa)] \ , \tag{4.4}$$

which satisfies (4.1) but not (4.2). The long wavelength limit of the relaxation time is given by (2.19)

$$\tau_S(0) = \beta m D. \tag{4.5}$$

Compared to (3.1) the assumption (4.4) is a simpler approximation. This is because J_t is a higher-order correlation function than S_S. In view of (2.20) the assumption of (4.4) is equivalent to the statement that $f(\omega)$ is a simple Lorentzian. From the results of computer molecular-dynamics experiment this is known to be a rather poor representation.[9,10] Although we will investigate the implications of (4.4), mainly because of its simplicity, it seems worthwhile to consider more sophisticated approximations.

On the basis of the computer $f(\omega)$ obtained by Rahman, we know that any reasonable approximation should show a resonant behavior at a nonzero frequency. Thus we might consider

$$D_S'(K,\omega) = a(\kappa)\tau_S(\kappa)/\{[\omega^2-\omega_0^2(\kappa)]^2+[\omega/\tau_S(\kappa)]^2\} \ , \tag{4.6}$$

a form which has been derived in the study of $f(\omega)$.[27,28] In order to satisfy (2.13), (4.1), and (4.2) we need to take

$$a(\kappa) = \omega_0^2(\kappa)/\beta m\tau_S^2(\kappa) \ , \tag{4.7}$$

$$\omega_0^2(\kappa) = 3\kappa^2/\beta m + (3m)^{-1}\langle \nabla^2\phi(r)\rangle \ , \tag{4.8}$$

$$\tau_S(0) = [\beta m D\omega_0^2(0)]^{-1} \ . \tag{4.9}$$

In the $\kappa = 0$ limit, (4.6) gives a qualitatively correct representation of the computer $f(\omega)$. Notice however that in this approximation $\tau_S(\kappa)$ is still undetermined. A simple approximation which enables us to utilize the sum rules to determine the relaxation time function is

$$D_S'(\kappa,\omega) = [b_0 + b_1(\kappa)\omega^2]\,\tau_S(\kappa)\,e^{-\omega^2\tau_S(\kappa)\pi}\ , \tag{4.10}$$

where upon using (2.19), (4.1), and (4.2) we find

$$b_0 = D/\tau_S(0), \tag{4.11}$$

$$b_1(\kappa) = (2/\pi)\tau_S^{\,2}(\kappa)\,[\,1/\beta m - D/\tau_S(0)\,] \tag{4.12}$$

and $$\tau_S^{\,2}(\kappa) = (\pi/2)[(3m)^{-1}\langle\nabla^2\phi(r)\rangle + 2\kappa^2/\beta m]^{-1}\ . \tag{4.13}$$

Thus with this approximation we have a complete specification of the damping function.

Computer calculations of $S_S(\kappa,\omega)$ for liquid argon at 85.5°K have been reported by Nijboer and Rahman.[10] At any fixed κ the function has a maximum at $\omega = 0$ and decays smoothly in a rather uninteresting manner. However, we can use the half-width at half-maximum of S_S to characterize the behavior of the self-correlation function. We shall denote this frequency by $\omega_{1/2}(\kappa)$. The computer half-width is shown in Fig. 5, where it is given in units of $D\kappa^2$. If the correlation function obeys a simple diffusion equation, then the reduced width would be unity for all κ. Notice that the half-width shows a dip around $\kappa \sim 2$, which is the position of the first maximum in the structure factor $S(\kappa)$. This behavior suggests that spatial correlation effects manifest even in a test-particle correlation function. Moreover, computer results indicate that the narrowing phenomenon is associated with the corrections to the so-called Gaussian approximation.[29]

As in Sec. III we can use the computer data to derive relaxation times corresponding to different approximations. Combining (2.12), (2.24), and (4.4) we have

$$S_S(\kappa,\omega) = \pi^{-1}[\,\kappa^2/\beta m\tau_S(\kappa)\,]/\{[\omega^2 - \kappa^2/\beta m)^2 + [\,\omega/\tau_S(\kappa)\,]^2\}, \tag{4.14}$$

from which we obtain the relation between $\tau_S(\kappa)$ and $\omega_{1/2}(\kappa)$,

$$\tau_S^{-2}(\kappa) = [\,(\kappa^2/\beta m)^2 + (2\kappa^2/\beta m)\omega_{1/2}^{\,2}(\kappa) - \omega_{1/2}^{\,4}(\kappa)\,]/\omega_{1/2}^{\,2}(\kappa)\ . \tag{4.15}$$

Using the computer curve in Fig. 5 we find the relaxation time labeled A in Fig. 6. The correlation function in the approximation (4.6) is

$$S_S(\kappa,\omega) = \frac{1}{\pi}\,\frac{\kappa^2 D_S'(\kappa,\omega)}{\left(\omega^2 - \dfrac{\omega\tau_S(\kappa)}{\omega_0^{\,2}(\kappa)}\,[\,\omega^2 + \omega_0^{\,2}(\kappa) + \tau_S^{-2}(\kappa)\,]\kappa^2 D_S'(\kappa,\omega)\right)^2 + [\,\kappa^2 D_S'(\kappa,\omega)]^2}\ , \tag{4.16}$$

which leads to a rather lengthy expression for $\tau_S(\kappa)$ in terms of $\omega_{1/2}(\kappa)$,

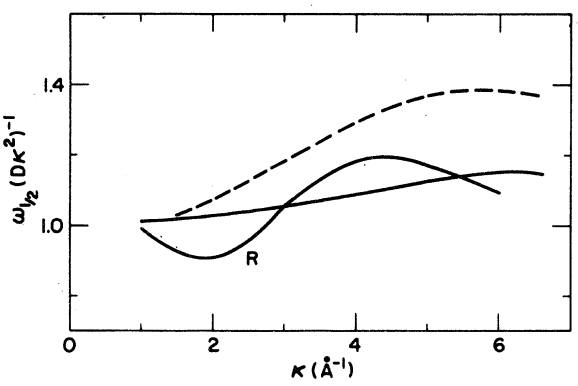

FIG. 5. Variation of half-width of $S_S(\kappa,\omega)$ with wave number, computer results (curve R), and calculations using (4.4) with constant τ_S at 1.06×10^{-13} sec (dashed curve) and using (4.10) (solid curve).

$$\tau_S^{-2}(\kappa) = \frac{2(\omega_0^2-\omega^2)[(\beta m\omega^2-\kappa^2)\beta m\omega_0^2\omega^2-(\beta m\omega^2-\kappa^2)^2\omega^2-(\omega_0^2-\omega^2)\kappa^4]+\kappa^4\omega_0^4+2\kappa^2\omega\sqrt{A}}{2\omega^2[2\kappa^4-(\beta m\omega^2-\kappa^2)^2]}\,, \tag{4.17}$$

where $A=(\beta m\omega_0^2-\kappa^2)^2\omega^6-2\omega_0^4(\beta^2m^2\omega_0^4-3\beta m\omega_0^2\kappa^2+3\kappa^4)\omega^4$

$$+\omega_0^4(\beta^2m^2\omega_0^4-3\beta m\omega_0^2\kappa^2+4\kappa^4)\omega^2+\omega_0^6\kappa^2(\beta m\omega_0^2-\kappa^2)\,. \tag{4.18}$$

The relaxation time function derived using (4.17) and the computer half-widths are labeled C in Fig. 6. The approximation (4.10) does not permit an analytic calculation of $\omega_{1/2}$ because the principal-value integral in $S_S(\kappa,\omega)$ has to be evaluated numerically. By trial and error we obtain the curve labeled B in Fig. 6 by requiring the calculated half-width to agree with Rahman's result.

It is interesting to observe that approximations (4.4) and (4.10) produced essentially the same relaxation time function, whereas (4.6) gave a quite different result. If one looks at the velocity autocorrelation function, (4.4) and (4.10) imply a structureless $f(\omega)$ whereas the $f(\omega)$ associated with (4.6) has a well-defined displaced peak. The fact that $\tau_S(\kappa)$ based on (4.6) is a much more smoothly behaved function suggests that (4.6) is a higher-order approximation. However, it should be noted that in this approximation $S_S(\kappa,\omega)$ is quite sensitive to the magnitude of $\tau_S(\kappa)$. In Fig. 5 we show the half-width obtained using (4.4) with $\tau_S(\kappa)$ equal to a constant (0.1063×10^{-12} sec), and that obtained using (4.10) with $\tau_S(\kappa)$ given by (4.13), the latter being a self-contained calculation based on (2.19) and the sum rules (4.1) and (4.2).

V. LONGITUDINAL CURRENT CORRELATION

By virtue of the continuity equation the longitudinal current correlation function $J_l(\kappa,\omega)$ and the density correlation function $S(\kappa,\omega)$ are simply related [compare (2.21)]. The results of this section are therefore also applicable to the analysis of neutron-scattering experiments, which we will discuss in the following section. The hydrodynamic behavior of J_l and S are quite well known.[2] For small κ and ω we know that $J_l(\kappa,\omega)$ is characterized by three hydrodynamic modes, a nonpropagating thermal conduction mode and two propagating sound modes. Martin has suggested that the simplest interpolation expression for the damping function, $D_l'(\kappa,\omega)$, which is consistent with the requirement of hydrodynamics, is[14]

$$D_l'(\kappa,\omega) = \frac{(\gamma-1)C_{l0}^2(0)/(\gamma D_T K^2)}{1+\omega^2/(\gamma D_T\kappa^2)^2} + \frac{(\frac{4}{3}\eta+\zeta)/mn}{1+\omega^2\tau_l^2(0)}\,, \tag{5.1}$$

where $\gamma=C_p/C_v$ is the ratio of specific heats, D_T is the thermal diffusivity, and $\tau_l(0)$ is a Maxwell relaxation time. We will assume that shear and volume viscous effects relax at the same rate and set $\tau_l(0)=\tau_t(0)$. With (5.1) one can satisfy (2.18) and the $\kappa=0$ limit of sum rule (2.13).

As a phenomenological extension we can modify (5.1) so that $D_l'(\kappa,\omega)$ satisfies (2.13) for all κ. In the spirit of the previous single relaxation-time approximations, we put

$$D_l'(\kappa,\omega) = \frac{a'(\kappa)\tau_l'(\kappa)}{1+\omega^2\tau_l'^2(\kappa)} + \frac{a(\kappa)\tau_l(\kappa)}{1+\omega^2\tau_l^2(\kappa)}\,, \tag{5.2}$$

where now because two processes are involved, the distribution of relative strengths is not uniquely determined. Notice that a straightforward generalization of (5.1) would result in

$$a(\kappa)=\langle\omega_l^2(\kappa)\rangle/\kappa^2-\gamma C_{l0}^2(\kappa)\,,$$

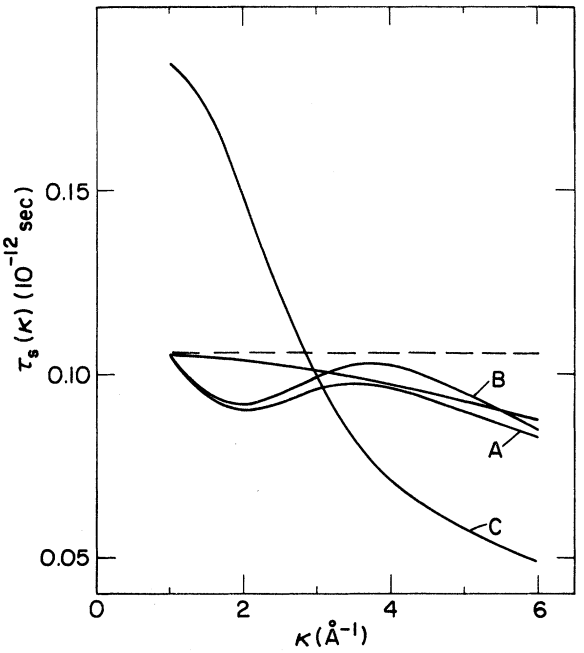

FIG. 6. Wave number dependence of the relaxation time $\tau_S(\kappa)$. Solid curve denotes (4.13) while dashed line is a constant at 0.106. Curves A, B, and C correspond to (4.15), (4.10), and (4.17), respectively. All the labeled curves will give the computer half-width shown in Fig. 5.

$$\tau_l(\kappa) = [\tau_l^{-1}(0) + \kappa V_0]^{-1} ,$$

$$a'(\kappa) = (\gamma - 1) C_{l0}^2(\kappa) , \tag{5.3}$$

$$\tau_l'(\kappa) = [1 + \gamma D_T \kappa / V_0] (\gamma D_T \kappa^2)^{-1} .$$

Alternatively we could require the relative strengths at $\kappa = 0$ be preserved for all κ,

$$a(\kappa)/a'(\kappa) = a(0)/a'(0) . \tag{5.4}$$

Condition (5.4) gives

$$a'(\kappa) = \frac{(\gamma - 1)\tau_l(0)\, C_{l0}^2(0)}{D_l + (\gamma - 1) C_{l0}^2(0) \tau_l(0)} \times [\langle \omega_l^2(\kappa)\rangle / \kappa^2 - C_{l0}^2(\kappa)] ,$$

$$a(\kappa) = \frac{D_l}{D_l + (\gamma - 1) C_{l0}^2(0) \tau_l(0)} \times [\langle \omega_l^2(\kappa)\rangle / \kappa^2 - C_{l0}^2(\kappa)] , \tag{5.5}$$

where $D_l = (\frac{4}{3}\eta + \zeta)/mn$. Despite the different appearances of $a(\kappa)$ and $a'(\kappa)$ in the two decompositions, the resulting damping functions differ very little because both must satisfy (2.13) or

$$a(\kappa) + a'(\kappa) = \langle \omega_l^2(\kappa)\rangle / \kappa^2 - C_{l0}^2(\kappa) . \tag{5.6}$$

The longitudinal current correlation function is given by

$$J_l(\kappa,\omega) = (\kappa^2/\beta m \pi)\, \kappa^2 D_l'(\kappa,\omega')\, \omega^2 \times \left[\left(\omega^2 - \frac{\kappa^2}{\beta m S(\kappa)} + \kappa^2 \omega^2 \mathcal{P} \int_{-\infty}^{\infty} \frac{d\omega'}{\pi} \frac{D_l'(\kappa,\omega')}{\omega'^2 - \omega^2} \right)^2 + [\omega \kappa^2 D_l'(\kappa,\omega)]^2 \right]^{-1} \tag{5.7}$$

With $D_l'(\kappa,\omega)$ given by (5.2) the principal-value integration is again easily carried out. Equation (5.7) is directly applicable to the analysis of computer data. The spectral densities of liquid argon at 76°K and density of 1.407 g/cm^3 as obtained by Rahman[12] are shown in Fig. 7. The solid curves denote Rahman's results and the crosses are values obtained using (5.2), (5.5), and (5.7). The parameters in this calculation are $D_T = 1.68 \times 10^{-3}$ cm^2/sec, $\gamma = 2.01$, and $\tau_l(0) = 1.35 \times 10^{-13}$ sec. The structure factor, $S(\kappa) = [\beta m C_{l0}^2(\kappa)]^{-1}$, and the sum rule $\langle \omega_l^2(\kappa)\rangle/\kappa^2$ are taken from Rahman's work. The agreement between theory and computer is generally satisfactory. Notice that the computer values do not vanish at $\omega = 0$ for κ around 2. This is a numerical inaccuracy since J_l must begin at the origin as can be seen from (5.7).

The peak position of $J_l(\kappa,\omega)$ as a function of κ is of interest because, roughly speaking, it represents a kind of dispersion relation of the liquid.[11,12] We shall denote this quantity as $(\omega_l)_{\max}$. In Fig. 8 the computer results[12] are given as solid circles while the crosses and other curves denote various theoretical estimates. It is well known that at small κ the dispersion relation of a liquid is linear in κ and its slope is simply the adiabatic sound speed, $\gamma C_{l0}(0)$. This is the hydrodynamic behavior of the longitudinal current correlation which can be derived from the linearized Navier-Stokes equations.[2] In the present approach the result also follows directly from (5.1). The thermal conduction term is important at small κ because if ignored one would obtain the isothermal sound speed instead.[14] As κ increases the computer results show a maximum in $(\omega_l)_{\max}$ followed by a minimum at the position where the structure factor has its first maximum. This type of behavior has been observed in several neutron scattering studies.[7,8] The computer results[12] also reveal the presence of a second maximum which occurs at about the position of the first minimum in $S(\kappa)$, and this too has been observed in the neutron data on liquid lead.[30]

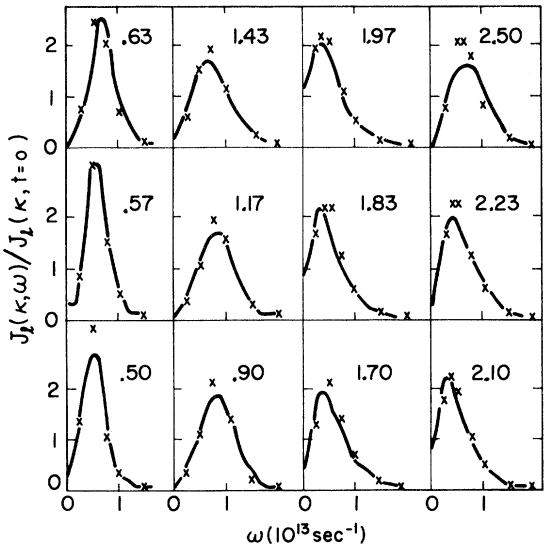

FIG. 7. Spectral densities of longitudinal current correlations in liquid argon (in units of 10^{-13} sec), with $J_l(\kappa, t=0) = \kappa^2/m\beta$. Solid curves are computer results while the crosses denote calculations using (5.5) and $\tau_l(\kappa)$ from (5.3). All curves have areas normalized to $\pi/2$.

The theoretical calculations shown in Fig. 7 give rise to a dispersion relation depicted by the solid curve in Fig. 8. There is at least a semiquantitative agreement with the computer data. The dashed curve corresponds to the same calculations except that a constant relaxation time (1.35×10^{-13} sec) was used for $\tau_l(\kappa)$. The difference is an indication of the sensitivity of $(\omega_l)_{\max}$ to $\tau_l(\kappa)$.

There are several approximate ways of estimating $(\omega_l)_{\max}$ analytically. A well-known result, based on sum rules and the assumption that $S(\kappa,\omega)$ and $J_l(\kappa,\omega)$ have single sharp peaks located at $\omega=(\omega_l)_{\max}$, is[31]

$$(\omega_l)_{\max}=\kappa[\beta m S(\kappa)]^{-1}\,, \tag{5.8}$$

which is represented by the curve B in Fig. 8. In terms of (5.7) the assumption is equivalent to saying that

$$C_{l0}^{\,2}(\kappa)\gg\omega D_l'(\kappa,\omega)\,. \tag{5.9}$$

The sum rules used to derive (5.8) are

$$\int_{-\infty}^{\infty}d\omega\, S(\kappa,\omega)=S(\kappa)\,, \tag{5.10}$$

$$\int_{-\infty}^{\infty}d\omega\, J_l(\kappa,\omega)=\kappa^2/\beta m\,. \tag{5.11}$$

One may also use the next-order sum rule, namely (2.13), and identify

$$(\omega_l)_{\max}=[\langle\omega_l^{\,2}(\kappa)\rangle]^{1/2}\,. \tag{5.12}$$

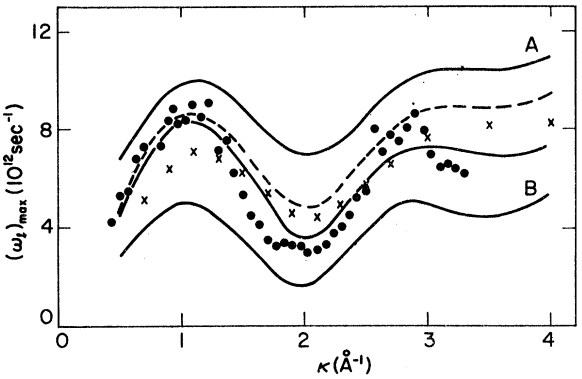

FIG. 8. Dispersion in excitation frequency of longitudinal current correlations in liquid argon. The points denote computer data while all others are theoretical results. Calculations using (5.5) and $\tau_l(\kappa)$ from (5.3) are shown as the solid curve while the same calculations using a constant $\tau_l(\kappa)$ at 1.35×10^{-13} sec appear as the dashed curve. The crosses are obtained from (5.15) with constant $\tau_l(\kappa)$, and curves A and B are obtained using (5.12) and (5.8), respectively.

This result, which has been discussed by Schofield[32] and derived by Nossal and Zwanzig,[33] is represented by the curve A in Fig. 8. Notice that if $S(\kappa,\omega)$ were a sharply peaked function of negligible width, (5.8) and (5.12) would lead to the same dispersion relation. The difference between curves A and B therefore reflects the fact that $J_l(\kappa,\omega)$ actually has considerable width, and this is what we have observed in Fig. 7.

In the opposite limit of large damping we can also obtain an analytic expression for $(\omega_l)_{\max}$. To simplify the algebra we consider only the viscous effects in (5.2) and write

$$D_l'(\kappa,\omega)=\frac{[\langle\omega_l^{\,2}(\kappa)\rangle/\kappa^2-C_{l0}^{\,2}(\kappa)]\,\tau_l(\kappa)}{1+\omega^2\tau_l^{\,2}(\kappa)}\,. \tag{5.13}$$

Inserting this into (5.7) and assuming

$$\omega D_l'(\kappa,\omega)\gg C_{l0}^{\,2}(\kappa)\,, \tag{5.14}$$

we obtain a cubic equation for $(\omega_l)_{\max}^{\,2}$. The physical solution gives

$$(\omega_l)_{\max}^{\,2}=\langle\omega_l^{\,2}(\kappa)\rangle-C_{l0}^{\,2}(\kappa)\kappa^2-\tfrac{1}{2}\tau_l^{\,-2}(\kappa)\,, \tag{5.15}$$

which may be compared with (3.7). If further we assume that $\tau_l(\kappa)$ is a constant at 1.35×10^{-13} sec we obtain the crosses shown in Fig. 8.

Finally we can infer from the computer data the relaxation time function appropriate to (5.2). The result obtained by interpolation is the curve labeled R′ in Fig. 9, where the transverse relaxation time is taken from Fig. 2. If approximations (3.1) and (5.2) are valid, and if shear and bulk viscous effects at finite κ[34] can be described by the same relaxation process, then R and R′ will be the same. The general behavior of the two functions are indeed similar, although R′ is smaller by about 20% and has a little more structure in the vicinity of the diffraction peak. The solid curve in Fig. 9 represents $\tau_l(\kappa)$ as assumed in (5.3) with $\tau_l(0)$ at 1.35×10^{-13} sec.

VI. INELASTIC NEUTRON SCATTERING

The preceding analyses have been primarily concerned with the behavior of various spectral densities in the range of κ of order Å^{-1} and ω of order 10^{12}–10^{13} sec^{-1}. In this region the density correlation functions $S(\kappa,\omega)$ and $S_s(\kappa,\omega)$ are directly measurable by inelastic neutron scattering; consequently our argon calculations can be used to discuss recent neutron experiments. The quantity which governs the scattering intensity is the double differential cross section,[28]

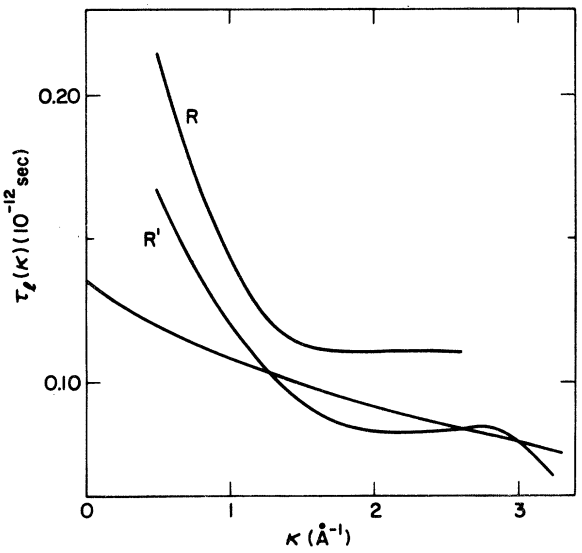

FIG. 9. Wave number dependence of the relaxation time $\tau_l(\kappa)$. Solid curve is from (5.3) with $\tau_l(0)$ at 1.35×10^{-13} sec while curve R' gives the best fit to computer $(\omega_l)_{\max}$ when used with (5.2) and (5.5). Curve R is taken from Fig. 2.

$$\frac{d^2\sigma}{d\Omega\,d\omega}=\frac{k_f}{k_i}\,e^{-\beta\hbar\omega/2}e^{-\beta\hbar^2\kappa^2/8m}\times[a_{\mathrm{coh}}{}^2S(\kappa,\omega)+a_{\mathrm{inc}}{}^2S_s(\kappa,\omega)]\ , \quad (6.1)$$

where k_i and k_f are the incident and scattered neutron wave numbers, $\hbar\vec{\kappa}=\hbar(\vec{k}_i-\vec{k}_f)$ and $\hbar\omega=\hbar(\omega_i-\omega_f)$ are neutron momentum and energy losses, and a_{coh} and a_{inc} are the coherent and incoherent scattering lengths. The two terms in (6.1) represent, respectively, the coherent and incoherent scattering contributions, both of which are important in the case of natural argon as $a_{\mathrm{coh}}{}^2=3.76\times10^{-26}$ cm^2 and $a_{\mathrm{inc}}{}^2=0.485\,a_{\mathrm{coh}}{}^2$. The density correlation function follows from (2.21) and (5.7)

$$S(\kappa,\omega)=(\pi\beta m)^{-1}\kappa^4D_l'(\kappa,\omega)\times\left[\left(\omega^2-\frac{\kappa^2}{\beta mS(\kappa)}+\omega^2\kappa^2\mathcal{P}\int_{-\infty}^{\infty}\frac{d\omega'}{\pi}\frac{D_l'(\kappa,\omega')}{\omega'^2-\omega^2}\right)^2+[\omega\kappa^2D_l'(\kappa,\omega)]^2\right]^{-1}\ , \quad (6.2)$$

where $D_l'(K,\omega)$ is given by (5.2) with $\tau_l(\kappa)$ given by (5.3) and $a(\kappa)$ and $a'(\kappa)$ given by (5.5). For the self-correlation function we have

$$S_s(\kappa,\omega)=\frac{\pi^{-1}\kappa^2D_s'(\kappa,\omega)}{\left(\omega+\omega\kappa^2\mathcal{P}\int_{-\infty}^{\infty}\frac{d\omega'}{\pi}\frac{D_s'(\kappa,\omega')}{\omega'^2-\omega^2}\right)^2+[\kappa^2D_s'(\kappa,\omega)]^2} \quad (6.3)$$

with $D_S'(\kappa,\omega)$ given by (4.10). The neutron-scattering intensity is thus completely specified in terms of sum rules (equilibrium properties) and transport coefficients.

In order to compare theory with experiment we first average (6.1) over an incident neutron spectrum assumed to be a normal distribution

$$F(\omega_i,\bar{\omega}_i)=(2\pi\sigma_i{}^2)^{-1/2}\exp\left[-\frac{1}{2}\left(\frac{\omega_i-\bar{\omega}_i}{\sigma_i}\right)^2\right] \quad (6.4)$$

with a standard deviation σ_i chosen to correspond to the actual experimental width. The scattering intensity then becomes

$$J(\kappa,\omega_f)=\int d\omega_i\frac{d^2\sigma}{d\Omega\,d\omega}F(\omega_i,\bar{\omega}_i)\ . \quad (6.5)$$

In addition there will be other corrections such as finite instrumental resolution effects and multiple scattering. We will assume these are small and can be neglected.

The spectra of neutrons inelastically scattered from liquid argon have been measured by Chen *et al.*[7] at 85 °K and by Sköld and Larsson[35] at 94.4 °K. Other measurements[36] also have been made, but they will not be considered here. The experimental data of Chen *et al.* were reported in the form of time-of-flight distributions, the conversion being

$$\frac{d^2\sigma}{d\Omega\,d\lambda}=\frac{4\pi\hbar^2\lambda_i}{m_n\lambda_f{}^4}\left(\frac{k_i}{k_f}\frac{d^2\sigma}{d\Omega\,d\omega}\right)\ , \quad (6.6)$$

where m_n is the neutron mass and $\lambda=2\pi/k$ is the wavelength. The parameters used in the theoretical calculations are listed in Table II. In addition, we have used the measured value[37] of $S(\kappa)$ at 84 °K without any temperature correction, and in computing $\langle\omega_l{}^2(\kappa)\rangle/\kappa^2$ we used the pair distribution functions $g_2(r)$ computed by Verlet[24] ($mn=1.42$ g/cm^3 and $T=86$ °K for the Chen experiment and $mn=1.374$ g/cm^3 and $T=94.4$ °K for the Sköld-Larsson experiment).

The observed and computed neutron spectra at fixed scattering angles are shown in Figs. 10 and 11. Also shown in Fig. 10 are the calculations of Desai and Nelkin[38] using computer data (mean-square displacement) to obtain $S_s(\kappa,\omega)$ and a phenomenological prescription (Delayed-Convolu-

tion Approximation) to obtain $S(\kappa,\omega)$. Sköld and Larsson have reported their data as constant-κ and constant-ω spectra. The variation of intensity with wavelength is shown in Fig. 12, where

TABLE II. Data and constants used in the analysis of neutron-scattering experiments on liquid argon.

		Chen *et al.*	Sköld-Larsson
T	(°K)	85	94.4
mn	(g/cm^3)	1.42	1.37
C_p/C_v		2.11	2.16
η	(10^{-3} g/cm sec)	2.16	2.16
D	(10^{-5} cm^2/sec)	1.88	2.43
D_T	(10^{-4} cm^2/sec)	8.06	8.14
$\tau_s(0)$	(10^{-12} sec)	0.106	0.124
$\tau_l(0)$	(10^{-12} sec)	0.128	0.12
$\bar{\omega}_i$	(10^{12} sec^{-1})	4.46	7.38
σ_i	(10^{12} sec^{-1})	0.314	0.684

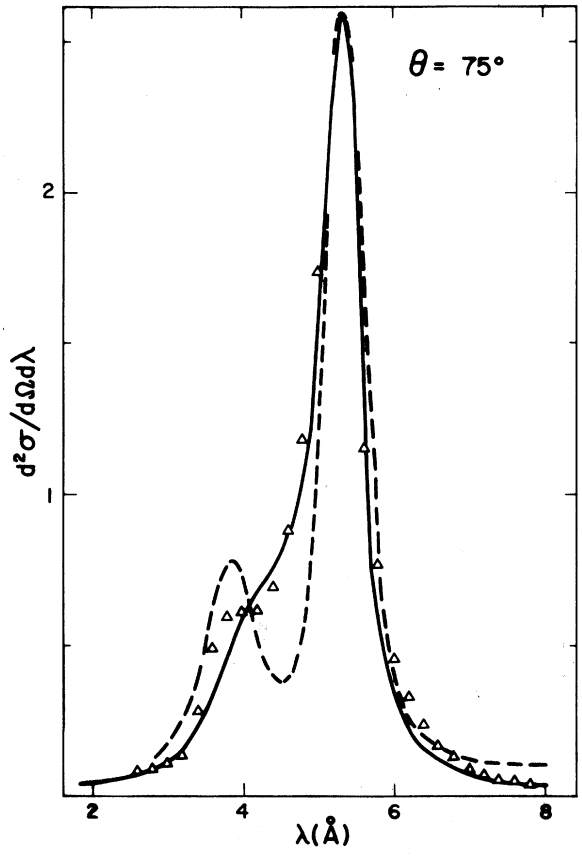

FIG. 10. Neutron-scattering intensity of liquid argon at 85°K (in units of 10^{-18} cm/sr atom) as a function of the wavelength of scattered neutrons and at $\theta=75°$, present calculations (solid), experimental data of Chen *et al.* (dashed), and Desai-Nelkin calculations (triangles). Theoretical spectra have been averaged over the incident neutron spectrum.

$\Delta\nu=(\omega_f-\omega_i)/2\pi$. The solid theoretical curves correspond to (6.5) with the cross section evaluated from (6.1) through (6.3). The dashed curves correspond to the same calculations except that $\tau_l(\kappa)$ has been treated as a constant (1.2×10^{-13} sec). It can be observed that variations in the relaxation time have considerable influence on the neutron spectra. Since one is comparing absolute intensities in Fig. 12, the agreement between *a priori* calculations and experiment is quite good. The variation of scattering intensity with frequency is not particularly interesting; however, if one plots the full width at half-maximum as a function of wave number, the behavior is that shown in Fig. 13. The narrowing phenomenon at the diffraction maximum was first predicted by deGennes[16] using sum rule arguments; more recently it has been discussed by Schofield.[32]

The dispersion relations extracted from the above experiments[7,39] are shown in Fig. 14 along with the theoretical results calculated at 94.4°K. The latter values are peak positions in $\omega^2S(\kappa,\omega)$ and are therefore the same as $(\omega_l)_{\max}$. We have

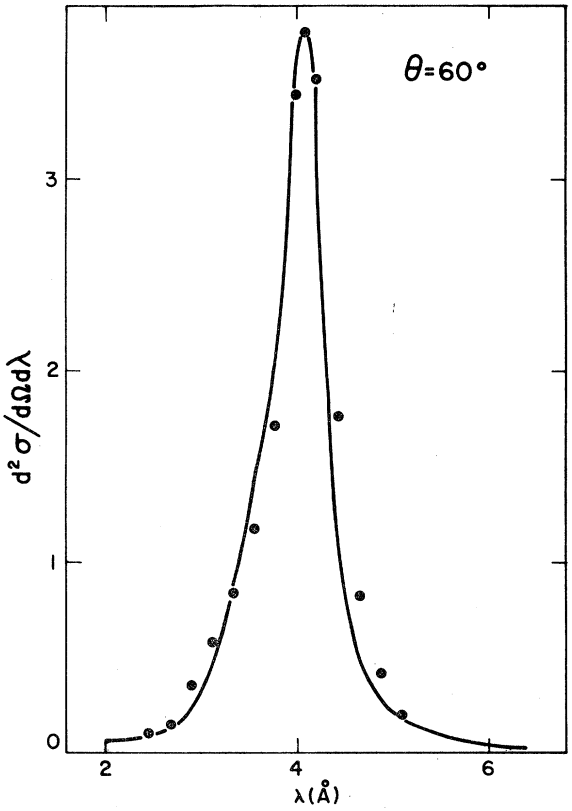

FIG. 11. Neutron-scattering intensity of liquid argon at 94.4°K (arbitrary units) as a function of wavelength and at $\theta=60°$, present calculations (solid curve) and experimental points of Sköld and Larsson (taken from Fig. 8 of Ref. 35). Theoretical results have been averaged over the incident neutron spectrum.

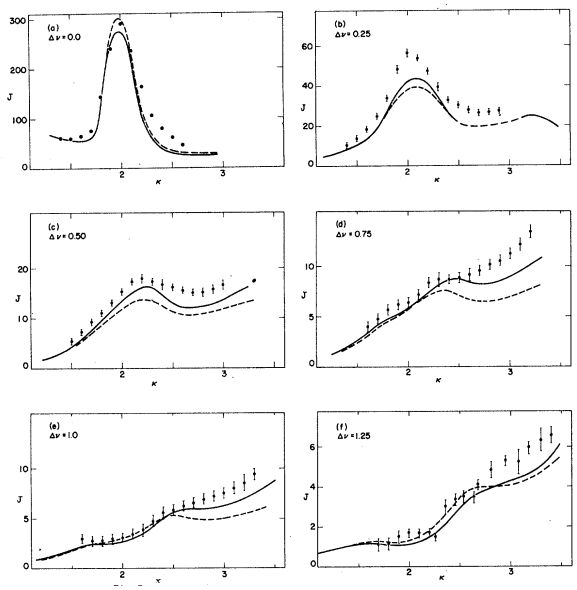

FIG. 12. Neutron-scattering intensity $J(\kappa, \omega_f)$ of liquid argon at 94.4°K [in units of 2.2×10^{-40} cm^2/(sr sec^{-1} atom)], experimental points of Skölds and Larsson and calculations with κ-dependent relaxation time (solid curves) and with a constant relaxation time (dashed curves).

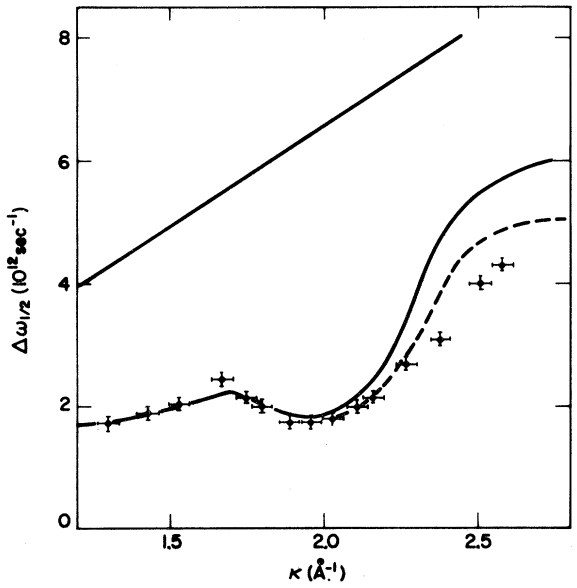

FIG. 13. Full width at half-maximum of $J(\kappa, \omega_f)$. Notations are same as Fig. 12, and the straight line denotes the ideal-gas result.

also examined the peak positions in

$$\omega^2[a^2_{\text{coh}} S(\kappa,\omega) + a^2_{\text{inc}} S_s(\kappa,\omega)]$$

and found that they agree with $(\omega_l)_{\max}$ to within a few percent. The reason that the incoherent

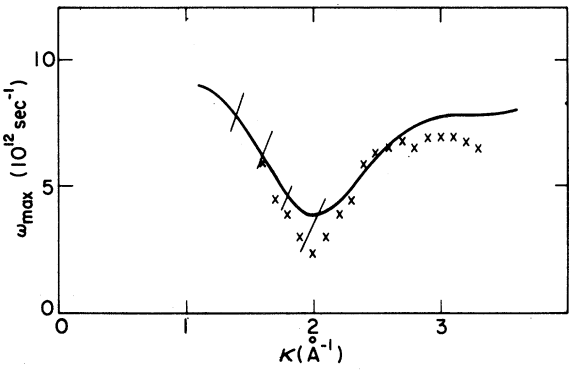

FIG. 14. Comparison of theoretical dispersion relation for liquid argon at 94.4°K with neutron data, Sköld-Larsson measurements at 94.4°K (crosses) and Chen *et al.* measurements at 85°K (bars).

contribution apparently has no effect is that $\omega^2 S_S(\kappa,\omega)$ gives a relatively very broad peak. By analyzing the peak position in $\omega^2 S_S(\kappa,\omega)$ we found that it increases monotonically with κ and is in fact quite similar to the ideal-gas result of $(2k_b T/m)^{1/2}\kappa$. It is perhaps interesting to note that at $\kappa \sim 2$ the theoretical frequency in Fig. 14 drops to a value about the same as that found from $\omega^2 S_S$, or from the above ideal-gas expression. The same behavior is also evident in the experimental dispersion curve of liquid lead obtained by Randolph.[30]

VII. DISCUSSIONS

In this work we have attempted to generalize the hydrodynamic expressions for correlation functions by using a frequency and wavelength-dependent damping function and by requiring that sum rules containing the two-particle equilibrium distribution function be satisfied. In the limit of long wavelengths and low frequencies the damping function, $D'(\kappa,\omega)$, is simply related to a transport coefficient or a linear combination of such coefficients. Its behavior at finite κ and ω is generally unknown, although its frequency moments can be specified in terms of the sum rules for the corresponding correlation function. By assuming simple frequency dependence in D' without regard to sum rules, one finds that in the transition region with κ of order Å^{-1} and ω of order 10^{12} sec^{-1} the damping effects are too large. However, if the damping function is also required to satisfy the sum rule which involves the equilibrium pair distribution function, the calculations then improve significantly. For example, in the case of density or longitudinal current correlation, the inclusion of κ-dependent shear and bulk mokuli in $D_l^l(\kappa,\omega)$ and the use of $[S(\kappa)]^{-1}$ as a generalized compressibility factor enable us

to reproduce all the qualitative features of the correlation functions as observed by computer experiments and neutron scattering. One may conclude that the elastic properties of a liquid have an important influence on its response in the transition region. Also much of the spatial correlation effects can be adequately treated through only the pair distribution function.

The results of computer molecular-dynamics experiments appear to be sufficiently precise to provide detailed information about the damping function. This may be seen from the fact that while a simple Lorentzian frequency dependence in $D'(\kappa,\omega)$ may be a useful approximation, it does not give a completely satisfactory representation of the computer results even when computer data are first used to determine the optimum relaxation time function. It would be important to know if the actual frequency dependence of $D'(\kappa,\omega)$ can be reasonably represented by a simple analytic expression. To study this problem one can reverse the calculation by expressing $D'(\kappa,\omega)$ in terms of the correlation function and using computer data to generate the damping function. This approach has been discussed for the velocity autocorrelation function of liquid argon, where D_S' has the interpretation of a frequency-dependent friction constant, and it was found that D_S' has a more smooth frequency variation than the correlation function itself.[40] Similar analysis using computer values of $S(\kappa,\omega)$, $J_t(\kappa,\omega)$, and $S_S(\kappa,\omega)$ would be of interest, and the results should be helpful in studying approximate methods for calculating $D'(\kappa,\omega)$. We note that one can also interpret D' as a memory function. This point of view has been applied mainly to the calculation of autocorrelation functions.[27,41]

In the case of van Hove self-correlation function, we have also considered a Gaussian frequency dependence for the damping function which may be regarded as the wavelength-dependent velocity autocorrelation function. The Gaussian assumption has the advantage in that sum rules corresponding to the fourth frequency moment of $S_S(\kappa,\omega)$ and higher can now be introduced.[42] Since the fourth moment can be easily computed, we have been able to construct a phenomenological $D_S'(\kappa,\omega)$ in a self-consistent way. This procedure gives the half-width of S_S in better agreement than that derived from the simple Lorentzian assumption with a constant relaxation time. The comparison is inconclusive, however, since any relaxation time function can be used with a Lorentzian $D'(\kappa,\omega)$. Indeed, we observe from the analysis of transverse current correlation that quite good results are obtained with an interpolation prescription for $\tau_t(\kappa)$ such as that proposed by Akcasu and Daniels.[25] Generally speaking, we can conclude that frequency and wavelength effects in $D'(\kappa,\omega)$ are not simply separable, so that any discussion of the relaxation time can be made only in the context of the assumed frequency dependence. Assumptions which lead to relaxation times having simple behavior provide useful calculational procedures, but the question of a κ-dependent relaxation time as a basic concept remains to be clarified.

Since the sum rules play an important role in the present calculations, one may question the utility of higher-order sum rules, such as $\langle\omega_l^4(\kappa)\rangle$, if they are available. The molecular expressions at finite κ have been derived but not evaluated because of computational difficulties. The same information can be obtained from the fourth-order time derivatives at $t=0$ of the time correlation functions generated by computer experiments. When these results are known, one may be able to completely specify the wavelength dependence of $D'(\kappa,\omega)$.

In the analysis of neutron-scattering experiments on liquids one of the difficulties has been a proper calculation of the coherent effects. An early procedure was to assume that $S(\kappa,\omega)$ can be computed using the structure factor $S(\kappa)$ and the self-correlation $S_S(\kappa,\omega)$. The Convolution approximation was first suggested by Vineyard,[29] and a number of modifications subsequently have been proposed.[6,9,16] The feature common to all the prescriptions is that the dynamics is treated in terms of a single-particle model, and because of this they all fail to give the proper hydrodynamic behavior at long wavelengths and low frequencies. The present approach does not suffer from this defect.[43] Regardless of the assumptions concerning the damping function or the relaxation time, all the correlation function expressions have the correct hydrodynamic limit. By making simple assumptions about $D_l'(\kappa,\omega)$ and $\tau_l(\kappa)$ we have been able to obtain, without any adjustable parameter, the absolute neutron-scattering intensities for argon which are in at least semiquantitative agreement with experiment. Since neutron data on liquid lead[8,44] and sodium[45] are available, it would be interesting to see if similar analysis is useful for liquid metals as well.[46]

ACKNOWLEDGMENTS

We would like to thank P. C. Martin and S. H. Chen for helpful discussions. Also we thank P. Schofield, Z. A. Akcasu, and R. Zwanzig for discussions and communication of their own related calculations prior to publication. This work was supported by the National Science Foundation under Grant No. GK-1721.

[1]R. Zwanzig, Ann. Rev. Phys. Chem. 16, 67 (1965); P. A. Egelstaff, Rept. Progr. Phys. 29, 333 (1966).

[2]P. C. Martin, in Many-Body Physics, eds. DeWitt and Balian (Gordon and Breach, Publishers, Inc., New York, 1968), p. 39; L. P. Kadanoff and P. C. Martin, Ann. Phys. (N. Y.) 24, 419 (1963).

[3]For a discussion of time correlations functions in molecular systems, see R. G. Gordon, in Advances in Magnetic Resonance, edited by J. S. Waugh (Academic Press Inc., New York, 1968), Vol. 3, p. 1.

[4]L. van Hove, Phys. Rev. 95, 249 (1954).

[5]P. A. Egelstaff, An Introduction to the Liquid State (Academic Press Inc., London, 1967).

[6]For a recent review see K. E. Larsson, in Neutron Inelastic Scattering (International Atomic Energy Agency, Vienna, 1968), Vol. 1, p. 397. Earlier reviews may be found in Thermal Neutron Scattering, edited by P. A. Egelstaff (Academic Press Inc., London, 1965), Chaps. 7 and 8.

[7]S. H. Chen, O. J. Eder, P. A. Egelstaff, B. C. G. Haywood, and F. J. Webb, Phys. Letters 19, 269 (1965).

[8]S. J. Cocking and P. A. Egelstaff, Phys. Letters 16, 130 (1965); P. D. Randolph and K. S. Singwi, Phys. Rev. 152, 99 (1966). For a recent discussion of dispersion curves in liquid metals, see S. J. Cocking, British Atomic Energy Research Establishment Report, R5867, 1968, available from Scientific Administration Office, AERE (unpublished), Harwell, Didcot, England.

[9]A. Rahman, Phys. Rev. 136, A405 (1964).

[10]B. R. A. Nijboer and A. Rahman, Physica 32, 415 (1966).

[11]A. Rahman, Phys. Rev. Letters 19, 420 (1967).

[12]A. Rahman, in Neutron Inelastic Scattering (International Atomic Energy Agency, Vienna, 1968), Vol. 1, p. 561.

[13]Similar analyses of computer experiments have been carried out independently by P. Schofield, by Z. Akcasu and E. Daniels, and by R. Zwanzig, N. Ailawadi and A. Rahman (private communication and work to be published).

[14]P. C. Martin, in Statistical Mechanics of Equilibrium and Non-Equilibrium, edited by J. Meixner (North-Holland Publishing Co., Amsterdam, 1965), p. 100.

[15]A lucid discussion of Martin's correlation function formalism is contained in the lectures of A. Sjölander, 2nd International Summer School in Solid State Physics, Herceg Novi, Yugoslavia, 1968 (to be published).

[16]P. G. deGennes, Physica 25, 825 (1959).

[17]D. Forster, P. C. Martin, and S. Yip, Phys. Rev. 170, 155 (1968), and references given therein.

[18]R. Zwanzig and R. D. Mountain, J. Chem. Phys. 43, 4464 (1965).

[19]P. Schofield, in Inelastic Scattering of Neutrons in Solids and Liquids (International Atomic Energy Agency, Vienna, 1961), p. 39; A. Rahman, K. S. Singwi, and A. Sjölander, Phys. Rev. 126, 986 (1962).

[20]R. Kubo, in Lectures in Theoretical Physics (Interscience Publishers Inc., New York, 1959); also R. Kubo, Rept. Progr. Phys. 29, 255 (1966), and references therein.

[21]R. D. Mountain and R. Zwanzig, J. Chem. Phys. 44, 2777 (1966). See also R. Zwanzig, *ibid.* 43, 714 (1965) for a discussion of frequency-dependent transport coefficients.

[22]D. Forster, P. C. Martin, and S. Yip, Phys. Rev. 170, 160 (1968).

[23]D. G. Naugle, J. H. Lunsford, and J. R. Singer, J. Chem. Phys. 45, 4669 (1966).

[24]We have computed numerically $\langle\omega_t^2(\kappa)\rangle/\kappa^2$ and $\langle\omega_l^2(\kappa)\rangle/\kappa^2$ for liquid argon at various densities and temperatures using the values of equilibrium pair distribution function from L. Verlet, Phys. Rev. 165, 201 (1968).

[25]Z. A. Akcasu and E. Daniels, to be published.

[26]R. Zwanzig, Phys. Rev. 133, A50 (1964) has discussed the relation between $S_s(\kappa,\omega)$ and a generalized self-diffusion coefficient.

[27]B. J. Berne, J. P. Boon, and S. A. Rice, J. Chem. Phys. 45, 1086 (1966).

[28]R. C Desai and S Yip, Phys. Rev. 166, 129 (1968). In Figs. 4 and 5 of this reference, the unit of $J(k_f\omega_f)$ should be 2.2×10^{-41} cm^2/(sr sec^{-1} atom).

[29]G. H. Vineyard, Phys. Rev. 110, 999 (1958).

[30]P. D. Randolph, Phys. Rev. Letters 20, 531 (1968).

[31]For example, D. Pines, The Many-Body Problem (W. A. Benjamin, Inc., New York, 1961), p. 81. See also the discussion of deGennes (Ref. 16) and of Egelstaff (Ref. 5, p. 193).

[32]P. Schofield, Proc. Phys. Soc. (London) 88, 149 (1966).

[33]R. Nossal and R. Zwanzig, Phys. Rev. 157, 120 (1967). Numerical results for liquid argon were first obtained by R. Nossal, Phys. Rev. 166, 81 (1968) using an approximate equilibrium pair correlation function.

[34]Relaxation times for volume viscosity at $\kappa=0$ have been obtained by R. D. Mountain (unpublished).

[35]K. Sköld and K. E. Larsson, Phys. Rev. 161, 102 (1967).

[36]N. Kroo, G. Borgonovi, and K. Sköld, Phys. Rev. Letters 12, 721 (1964); B. A. Dasannacharya and K. R. Rao, Phys. Rev. 137, A417 (1965).

[37]D. G. Henshaw, Phys. Rev. 105, 976 (1957).

[38]R. C. Desai and M. Nelkin, Phys. Rev. Letters 16, 839 (1966).

[39]K. S. Singwi, K. Sköld, and M. P. Tosi, Phys. Rev. Letters 21, 881 (1968).

[40]P. C. Martin and S. Yip, Phys. Rev. 170, 151 (1968).

[41]K. S. Singwi and A. Sjölander, Phys. Rev. 167, 152 (1968); W. C. Kerr, *ibid.*, 174, 316 (1968); L. Glass and S. A. Rice, *ibid.*, 176, 239 (1968).

[42]Gaussian damping function has been discussed by K. S. Singwi and M. P. Tosi, Phys. Rev. 157, 153 (1967); see also Ref. 40.

[43]The first attempt to apply Martin's correlation function formalism to neutron scattering was made by P. A. Egelstaff, Brit. J. Appl. Phys. 16, 1219 (1965), and also Ref. 5. Other attempts to compute $S(\kappa,\omega)$ directly have been made, see, for example, J. H. Ferziger and D. L. Feinstein, Phys. Rev. 158, 97 (1967); M. Nelkin and S. Ranganathan, *ibid.* 154, 222 (1967); S. J. Cocking and P. A. Egelstaff, J. Phys. C 1, 507 (1968).

[44]S. J. Cocking and P. A. Egelstaff, J. Phys. C 1, 507 (1968); G. D. Wignall and P. A. Egelstaff, *ibid.* 1, 519 (1968).

[45]P. D. Randolph, Phys. Rev. 134, A1238 (1964); S. J. Cocking, Ref. 8.

[46]For recent analyses of liquid metals data, see S. J. Cocking, in Neutron Inelastic Scattering (International Atomic Energy Agency, Vienna, 1968), Vol. 1, p. 463; R. C. Desai and S. Yip, Phys. Rev. 180, 299 (1969).

PHYSICAL REVIEW VOLUME 182, NUMBER 1 5 JUNE 1969

Replacement Factor in a Linear Chain

J. Lothe

Fysisk Institutt, Blindern Universitet, Oslo, Norway

and

G. M. Pound

Materials Science Department, Stanford University, Stanford, California 94305

(Received 26 September 1968)

A harmonic analysis of linear chains in terms of the classical phase integral was conducted in order to calculate the replacement factor, i.e., the partition function for the internal degrees of freedom that an isolated segment does not have because it is not part of an infinite chain. The replacement free energy is given by

$$F_n(\text{rep}) = -kT \ln(kT\sqrt{n}/\hbar\omega_D),$$

where n is the number of atoms in the segment and ω_D is the Debye frequency. It is concluded that the replacement factor is correctly calculated in terms of center-of-mass motions of segments *only* by considering just those contributions for which the internal cluster coordinates remain fixed.

INTRODUCTION

In the theory of nucleation in phase transitions it is customary to represent the internal free energy of formation of the embryos and critical nuclei in terms of macroscopic thermodynamic properties, such as volume free energy, and surface tension of the bulk stable phase.[1–3] It is important to know the limitations of this description and the order of magnitude of the correction factors involved. Among other things, one wants to calculate the free energy that a small cluster or nucleus (containing of the order of 100 molecules) does not have because it is not part of the bulk phase. The partition function for the six degrees of freedom that are missing in the isolated cluster is called the replacement factor.[4–6] The replacement factor has been alternatively described as the partition function for the six degrees of freedom in bulk that are replaced by free translation and rotation of the cluster.[2,4,7] Early attempts at handling this problem have been reviewed and discussed by Feder *et al.*[8] Recently, on the basis of qualitative considerations, Lothe and Pound[4] concluded that the replacement factor could best be represented by the partition function of the six degrees of freedom for translational and torsional motion of clusters in bulk relative to each other, with the internal coordinates of the clusters remaining fixed. The purpose of this paper is to check out this prescription against exact calculations for linear chains. It will turn out that the above prescription for the replacement factor is exact for the linear chain and that alternative procedures, which also recently have been proposed,[9] are wrong and involve inconsistencies.[6]

The infinite chain (bulk) will be mathematically divided into equal segments (clusters in bulk), and orthogonal transformations will be introduced that separate the partition function for the system into center-of-mass parts (replacement terms) and internal parts (free cluster parts). The results are finally tested by combining the replacement term and the internal term to give the known free energy per segment in the infinite chain. The treatment is a generalization of preliminary work in a Debye